Unified Power Quality Conditioner based on an Indirect Matrix Converter with a PV panel

Nathan Araujo, *Student, IST*

***Abstract*— The main goal of this master thesis is to propose a Unified Power Quality Conditioner (UPQC) that allows the connection of a photovoltaic panel to the grid without increase the number of power electronic converters.**

The proposed UPQC is based on an IMC, providing a DC link to connect the panel, through an inductive filter.

The connection to the grid is made by a series transformer, while the PCC connection is made in shunt.

Second order filters are used to minimize high frequency harmonics, generated by the switching of the semiconductors, in the series transformer and PCC connections. It is also sized the inductive filter to connect the PV.

The control of the converter is performed with the Sliding Mode Control Method, associated to state-space vectors representation, guaranteeing fast response times.

The PI controllers used to control the series transformer voltages and PV current are sized accordingly to the system dynamics.

Using MATLAB/Simulink for tests, results show improvement in the power factor and current THD, while the PCC voltages are maintained in situations of sag and swell and simultaneously provides the PV a connection to the grid, proving the power quality improvement with the UPQC, and it's use as a converter for the connection of a PV to the grid.

***Index Terms*—Active Power Filter, Power Quality, Unified Power Quality Conditioner, Indirect Matrix Converter, Sliding Mode Control, Photovoltaic Panel**

I. Introduction

With the increasing use of electronic equipment, Power Quality (PQ) has become an important subject, as most of these equipment is sensitive to grid disturbances. However, they are also responsible for the introduction of harmonics in the grid, thus decreasing PQ.

To overcome these problems different methods were developed, mainly UPQCs, shunt, series and hybrid active power filters (APFs), and Dynamic Voltage Restorers (DVR). Although APFs have higher cost and complex control, they have a better performance than passive filters [1]. While APFs can be placed in shunt, only for compensating harmonic currents or load unbalances and load reactive power compensation, or in series, compensating harmonic currents, load unbalances, and reactive power of the load, an UPQC system combine both functionalities [2].

The UPQC proposed in this paper is composed by two APFs in a back-to-back configuration without energy storage components, that is implemented based on an IMC, where the series APF is connected to the grid by a transformer and the shunt APF is directly connected.

With the increase of renewable energy sources for the typical consumer, the ones that have a need for an UPQC based on a configuration with a DC Link available, can use it to connect a PV to the PCC, making the system more cost-benefit.

II. Proposed UPQC system

The system is composed by a series transformer, the AC/DC/AC converter, a LC filter for the inverter and another for the rectifier, and an inductive filter for the PV.

A. Topology description

As the UPQC compensates the voltage and current harmonics and the voltage issues related to the grid, it is necessary to generate references in a way that the controllers are able to react. It's also necessary to maintain the current in the PV almost constant, as it manages the production of power by the Maximum Power Point Tracking (MPPT).

To control the voltage in the PCC, it's required that the transformer voltage, imposed by the inverter, compensates the anomalies in the grid voltage.

$$v_{transf} = v_{grid} - v_{load} \tag{1}$$

The reference to the grid currents are obtained by (2), and are used by the rectifier to compensate the harmonics introduced by the load.

$$i_{grid} = i_{conv} - i_{load} \tag{2}$$

The DC Link current in the rectifier is given by (3), where I'_{dc} is the current that flows through the inverter.

$$I_{dc} = I_{pv} - I'_{dc} \tag{3}$$

Generally, the power produced by the PV flows through the rectifier, unless there is an anomaly in the grid voltage.

B. Indirect Matrix Converter

The IMC is implemented as a combination of a rectifier and an inverter, as shown in Fig. 2. This topology implies a fixed voltage polarity because of the diodes [3], which is required for the connection of the PV, thus not proving a disadvantage.

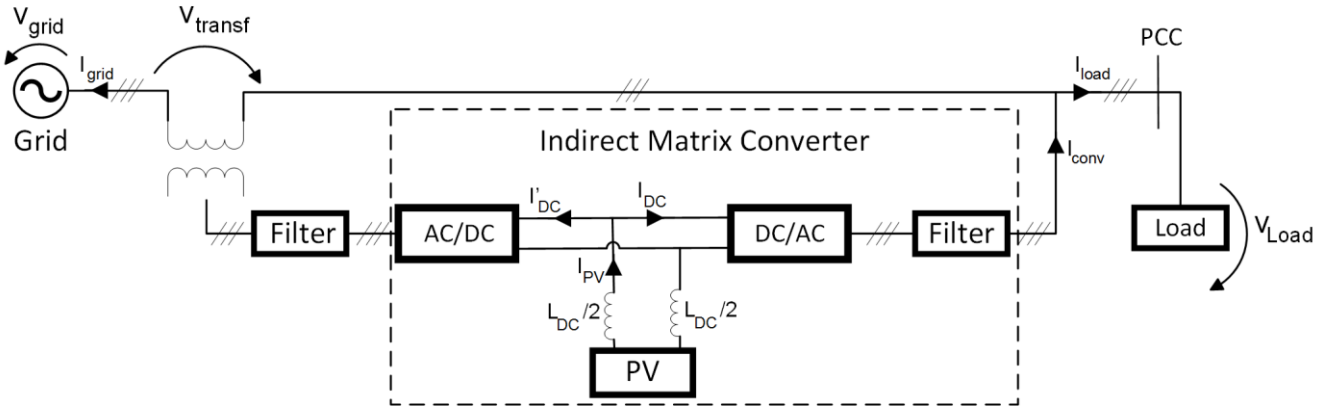

Figure 1. Unified Power Quality Conditioner with the PV inserted in the DC Link

Modelling the rectifier and the inverter by the matrix described in (4), the voltages and currents can be described as (5) for the rectifier and (6) for the inverter.

$$\mathbf{S_R} = \begin{bmatrix} S_{R_{11}} & S_{R_{12}} & S_{R_{13}} \\ S_{R_{21}} & S_{R_{22}} & S_{R_{23}} \end{bmatrix}$$
$$\mathbf{S_I} = \begin{bmatrix} S_{I_{11}} & S_{I_{21}} & S_{I_{31}} \\ S_{I_{21}} & S_{I_{22}} & S_{I_{23}} \end{bmatrix} = [\gamma_1 \quad \gamma_2 \quad \gamma_3] \tag{4}$$

$$v_{DC} = [S_{R_{11}} - S_{R_{21}} \quad S_{R_{12}} - S_{R_{22}} \quad S_{R_{13}} - S_{R_{23}}] \begin{bmatrix} v_a \\ v_b \\ v_c \end{bmatrix}$$
$$[i_a \quad i_b \quad i_c]^T = \mathbf{S_R}^{\mathrm{T}} \begin{bmatrix} i_{DC} \\ -i_{DC} \end{bmatrix} \tag{5}$$

$$\begin{bmatrix} v_{AB} \\ v_{BC} \\ v_{CA} \end{bmatrix} = [2\gamma_1 - 1 \quad 2\gamma_2 - 1 \quad 2\gamma_3 - 1]^T v_{DC}$$
$$i_{DC} = \mathbf{S_I}[i_a \quad i_b \quad i_c]^T \tag{6}$$

The switching states obtained for the rectifier and the inverter are represented in Table I, respectively.

III. Indirect Matrix Converter Modulation

To modulate the IMC, it is used the Space Vector Modulation (SVM), where the vectors are represented in a $\alpha\beta$ plane, using the power–invariant Concordia transformation. By doing this, it is possible to obtain vector references in a simpler way than using a abc plane.

The references are obtained considering the IMC divided in two parts, where the references for the AC voltage is set by the inverter and the AC current by the rectifier.

A. Rectifier

As the PV always injects power through the rectifier, the DC current I_{DC} is not be negative, and by applying the Concordia transformation, the absolute value and argument are the ones in Table I, and the vectors in the $\alpha\beta$ plane as shown in Fig. 3.

B. Inverter

The modulation of the inverter always considers a positive voltage in the DC link V_{DC}, as it is necessary for the implementation of the IMC and the PV. In the same way as the rectifier the voltage is given by Table II, in absolute value and argument in the $\alpha\beta$ plane, and the vectors as shown in Fig. 4.

IV. Control of the System

The control of the IMC is done using the sliding mode control [4][5]. This method of non-linear control implies a more complex filter and the need of more information from the

TABLE I. SWITCHING STATES OF THE RECTIFIER WITH THE SWITCHES CONDUCTING ON THE UPPER **(1)** AND LOWER **(2)** BRANCHES

S	(1)	(2)	v_{DC}	i_a	i_b	i_c	$\lvert I\rvert$	μ
R_1	$S_{R_{11}}$	$S_{R_{23}}$	$-v_{ca}$	i_{DC}	0	$-i_{DC}$	$\sqrt{2}i_{DC}$	$\pi/6$
R_2	$S_{R_{12}}$	$S_{R_{23}}$	v_{bc}	0	i_{DC}	$-i_{DC}$	$\sqrt{2}i_{DC}$	$\pi/2$
R_3	$S_{R_{12}}$	$S_{R_{21}}$	$-v_{ab}$	$-i_{DC}$	i_{DC}	0	$\sqrt{2}i_{DC}$	$5\pi/6$
R_4	$S_{R_{13}}$	$S_{R_{21}}$	v_{ca}	$-i_{DC}$	0	i_{DC}	$\sqrt{2}i_{DC}$	$-5\pi/6$
R_5	$S_{R_{13}}$	$S_{R_{22}}$	$-v_{bc}$	0	$-i_{DC}$	i_{DC}	$\sqrt{2}i_{DC}$	$-\pi/2$
R_6	$S_{R_{11}}$	$S_{R_{22}}$	v_{ab}	i_{DC}	$-i_{DC}$	0	$\sqrt{2}i_{DC}$	$-\pi/6$
R_7	$S_{R_{11}}$	$S_{R_{21}}$	0	0	0	0	-	-
R_8	$S_{R_{12}}$	$S_{R_{22}}$	0	0	0	0	-	-
R_9	$S_{R_{13}}$	$S_{R_{23}}$	0	0	0	0	-	-

TABLE II. SWITCHING STATES OF THE INVERTER

S	γ_1	γ_2	γ_3	v_{AB}	v_{BC}	v_{CA}	i_{DC}	$\lvert V\rvert$	δ
I_1	1	0	0	v_{DC}	0	$-v_{DC}$	i_A	$\sqrt{2}v_{DC}$	$\pi/6$
I_2	1	1	0	0	v_{DC}	$-v_{DC}$	$-i_C$	$\sqrt{2}v_{DC}$	$\pi/2$
I_3	0	1	1	$-v_{DC}$	v_{DC}	0	i_B	$\sqrt{2}v_{DC}$	$5\pi/6$
I_4	0	1	1	$-v_{DC}$	0	v_{DC}	$-i_A$	$\sqrt{2}v_{DC}$	$-5\pi/6$
I_5	0	0	1	0	$-v_{DC}$	v_{DC}	i_C	$\sqrt{2}v_{DC}$	$-\pi/2$
I_6	1	0	1	v_{DC}	$-v_{DC}$	0	$-i_B$	$\sqrt{2}v_{DC}$	$-\pi/6$
I_7	0	0	0	0	0	0	0	0	-
I_8	1	1	1	0	0	0	0	0	-

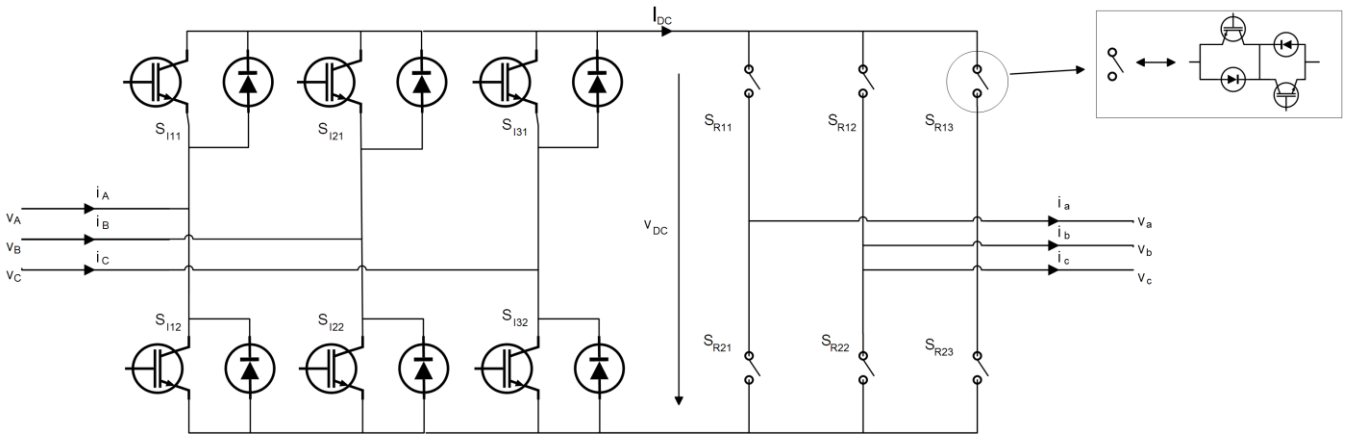

Figure 2. Topology of the Indirect Matrix Converter

system, although it allows a decrease of the system order and a quicker dynamic compared to linear controllers [6]. The commutation of the semiconductors is made in a way that the controlled parameter follows the reference.

A. *Rectifier Control*

The rectifier is controlled in a way that the current in the grid is in phase with the voltage and the power factor (PF) is nearly unitary, compensating the distortions caused by the load. Which means, in a dq plane, given by Park-Concordia transformation, de q component of the current is approximately zero, and the d component is given by the load and the PV current. This results in a PI controller that gives the reference for the current as shown in Fig. 5, from which the closed loop transfer function can be obtained in the canonical form (7) where $K_D = V_{DC}/I_{grid_d} = V_{grid_d}/I_{DC}$.

$$\frac{i_{DC}(s)}{i_{DC_{ref}}(s)} = \frac{\frac{K_D}{T_{di}L_{DC}}(sK_{Pi} + K_{ii})}{s^3 + \frac{1}{T_{di}}s^2 + \frac{K_{pi}K_D\alpha_i}{T_{di}L_{DC}}s + \frac{K_{ii}K_D\alpha_i}{T_{di}L_{DC}}} \quad (7)$$

Using Symmetric Optimum Method [7], the values of the proportional and integral gains, K_{pv} and K_{iv} are given by (8).

$$K_{pi} = \frac{L_{DC}}{K_D\alpha_i T_{di}a_i} \quad K_{ii} = \frac{L_{DC}}{K_D\alpha_i T_{di}^2 a_i^3} \quad (8)$$

Based on the dynamics of the system, the control of the grid currents implies a control of the DC Link voltage V_{DC}, which allows also the control of the PV current I_{PV} (9).

$$\frac{dI_{PV}}{dt} = \frac{V_{DC}}{L_{dc}} - \frac{V_{PV}}{L_{dc}} \quad (9)$$

B. *Inverter Control*

The inverter controls the transformer voltage, which indirect controls the PCC voltage, compensating for harmonic distortions, sags or swells, making the voltage applied to the load always sinusoidal and within the pre-determined values.

To control the voltage in the transformer, it is controlled the voltage in the capacitor of the LC filter as shown in Fig. 7, making it necessary a PI controller to give references to the AC current of the inverter.

Based on this scheme, the dynamics of the capacitor voltage (10) are obtained in a dq reference frame synchronized to the

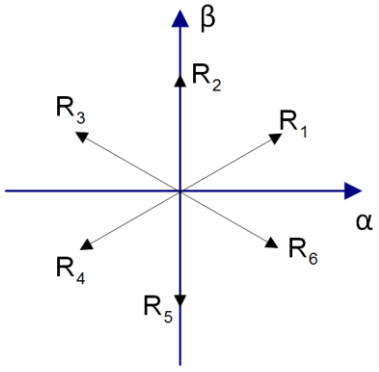

Figure 3. Current space vectors of the Rectifier

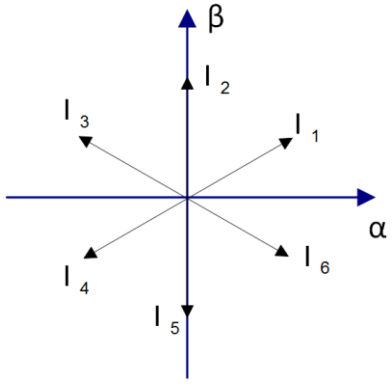

Figure 4. Voltage space vectors of the Inverter

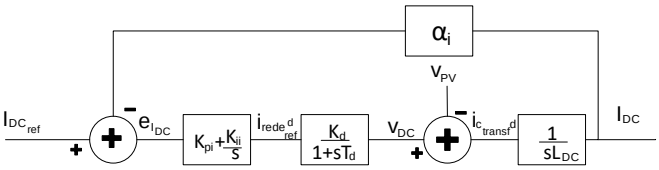

Figure 5. Block Diagram of the current Controller

output grid voltages.

$$\begin{cases} \dfrac{dv_{C_{trasnf}d}}{dt} = \dfrac{i_{inv_d}}{\sqrt{3}C_{transf}} - \dfrac{i_{transf_d}}{C_{transf}} + \omega_0 v_{C_{transf}q} \\ \dfrac{dv_{C_{trasnf}q}}{dt} = \dfrac{i_{inv_q}}{\sqrt{3}C_{transf}} - \dfrac{i_{transf_q}}{C_{transf}} - \omega_0 v_{C_{trasnf}d} \end{cases} \quad (10)$$

As there is a coupling of d and q, auxiliary variables H_{vd} and H_{vq} are defined (11).

$$\begin{cases} H_{vd} = \sqrt{3}\omega_0 C_{transf} v_{C_{trasnf}q} \\ H_{vq} = -\sqrt{3}\omega_0 C_{transf} v_{C_{trasnf}d} \end{cases} \quad (11)$$

Based on (10), (11) and Fig. 7, the block diagram of the voltage controller is obtained (Fig. 8). From Fig. 8, the closed loop transfer function is obtained in the canonical form (12)

$$\frac{v_{C_{transf_{dq}}}(s)}{v_{C_{transf}dq_{ref}}(s)} = \frac{\dfrac{(sK_{Pv} + K_{iv})\alpha_v}{T_{dv}C_{transf}n}}{s^3 + \dfrac{1}{T_{dv}}s^2 + \dfrac{K_{Pv}\alpha_v}{T_{dv}C_{trasnf}n}s + \dfrac{K_{iv}\alpha_v}{T_{dv}C_{transf}n}} \quad (12)$$

Using Symmetric Optimum Method [7], the values of the proportional and integral gains, K_{pv} and K_{iv} are given by (13).

$$K_{pv} = \frac{C_{transf}\alpha_i n}{\alpha_v T_{dv} a_v} \quad K_{iv} = \frac{C_{transf}\alpha_i n}{\alpha_v T_{dv}^2 a_v^3} \quad (13)$$

V. FILTER SIZING

To minimize the high frequency harmonics generated by the semiconductor switching, two second order LC filters are used, one connecting the inverter to the transformer and another between the rectifier and the PCC. Also it is necessary a L filter for the PV in order to adapt voltages and currents.

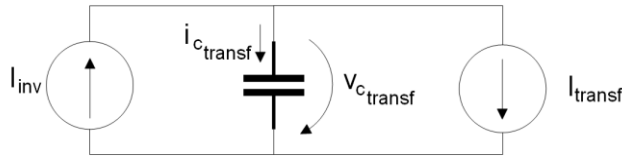

Figure 7. Simplified scheme used on the load voltage regulator

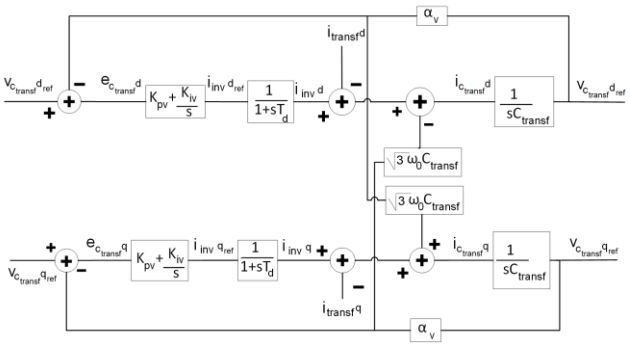

Figure 8. Block Diagram of the voltage Controller

A. *Inverter output filter*

The filter is sized based on the single-phase equivalent represented in Fig. 6, requiring the properly adaptation of the values for the type of connection and the side of the transformer where the filter is installed.

The inductance L_{transf} is given by (14), where Δi_L is the variation of the current in the inductor and f_s is the switching frequency.

$$L_{transf} = \frac{V_{DC}}{6\Delta i_L f_s} \quad (14)$$

Defining a cutoff frequency of the output filter (f_{co}),which generally is considered one frequency below the switching frequency and one decade above the grid frequency (f), the capacitor is given by (15).

$$C_{transf_{star}} = \frac{1}{4\pi^2 f_c^2 L_{transf}} \quad (15)$$

B. *Rectifier input filter*

Knowing the power that flows through the converter (P_{out}), the input voltage (V_i), and the grid angular frequency (ω) the value of the capacitor C_f for a given PF is obtained from (16).

$$C_f = \frac{P_{out}}{\omega V_i^2}\tan(\cos^{-1}(FP)) \quad (16)$$

Choosing the cutoff frequency of the input filter (f_{ci}), one decade below the switching frequency (f_s) and one decade

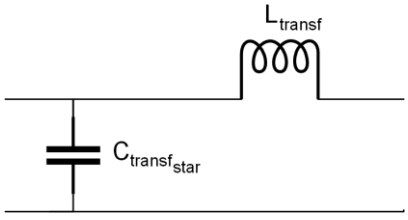

Figure 6. Single phase scheme of the input filter

above the grid frequency (f). The filter inductor L_f is sized according to (17).

$$L_f = \frac{1}{4\pi^2 f_{ci}^2 C_f} \tag{17}$$

To reduce the LC filter oscillations, a damping resistance r_p is connected in parallel to the inductor L_f. This resistance is calculated based on a negative incremental resistance r_i that is given by (18), where r_o is the equivalent output resistance and η is the converter efficiency [8].

$$r_i = -\frac{4}{3} r_o \eta \tag{18}$$

Knowing the characteristic impedance of the filter $Z_f = \sqrt{L_f / C_f}$ and the damping factor ξ, r_p is given by (19).

$$r_p = \frac{r_i Z_f}{2\xi r_i - Z_f} \tag{19}$$

C. PV filter

Knowing the voltage $v_{L_{DC}}$ (20) in the inductance L_{DC}, and considering Δt half of the switching frequency (f_s), the value of the inductance is obtained from (21).

$$v_{L_{DC}} = v_{DC} - v_{PV} = L_{DC} \frac{di_{L_{DC}}}{dt} \cong L_{DC} \frac{\Delta i_{L_{DC}}}{\Delta t} \tag{20}$$

$$L_{DC} = \frac{v_{DC} - v_{PV}}{2 f_s \Delta i_{L_{DC}}} \tag{21}$$

As the inductance is not ideal, the losses can be estimated by (22).

$$R_{DC} = \frac{P_{perdas}}{I_{L_{DC}}^2} \tag{22}$$

The values of the parameters are presented in section 6.

VI. Simulations Results

The system showed in Fig. 1 was simulated in MATLAB/Simulink, with the parameter values in Table III. These simulations aim to confirm the proper operation of the proposed system in two power quality disturbances (sags and swells). The PV is considered to work at Maximum Power Point (MPP) in rated conditions, with a current $I_{PV} = 15\text{A}$ and a voltage $V_{PV} = 240\text{V}$, considering an irradiance of 1000W/m^2 and ambient temperature of 25ºC.

The loads connected at the PCC are distributed evenly between linear and non-linear loads, with a total power of 720VA. The non-linear loads are simulated using a three-phase full-bridge diode rectifier.

The THD of the grid voltage and current in nominal condition are 2.25% and 6.48%, while the load current THD is 26.52%.

A. Power Quality Disturbances

The disturbances in the grid are shown in Fig. 9a, with a 20% sag beginning in $t = 0.625\text{s}$ and a 15% swell in $t = 0.775\text{s}$, both with a duration of 5 grid periods. The loads in Fig. 9b, shows that although there is a variation in the voltage, it is compensated. During the disturbances, the load voltages THD are 2.80% and 2.61%, for the sag and swell respectively. While the grid currents THD are 6.31% (sag) and 6.54% (swell).

B. PV parameters variance

A simulation is also made to confirm that the system can react to variations of the voltage and current resulting from the change of ambient temperature and irradiance. As shown in Fig. 10c, the grid current changes and stabilize in less than one grid period.

C. Simulation with another load

To guarantee the proper operation when a load has more power than the PV, resulting in power consumed from the grid, it was also simulated a situation where the load has a total power of 4.32 kW. Resulting in a THD of the voltage and the current of 2.56% and 5.41%.

TABLE III. SIMULATION PARAMETERS

Symbol	Description	Value
T_s	Sample time	4.9 µs
V	Grid phase to ground voltage (RMS value)	230 V
f_s	Switching frequency of the IMC	2 kHz
n	Series transformer turns ratio	1: 2
P_{PV}	PV nominal power	3.6 kW
L_{DC}	PV filter inductance	26.7 mH
R_{DC}	Inductance equivalent resistance	0.192 Ω
L_{transf}	Inverter filter inductance	16 mH
C_{transf}	Inverter filter line-to-line capacitance (Δ)	8.46 µF
L_f	Rectifier filter inductance	4.63 mH
C_f	Rectifier filter line-to-line capacitance (Δ)	6.03 µF
r_p	Rectifier filter resistance	36 Ω
α_i	Gain of the current sensor	1
α_v	Gain of the voltage sensor	1
K_{iv}	Voltage controller Integral Gain	8.46
K_{pv}	Voltage controller Proportional Gain	0.0085
K_{ii}	Current controller Integral Gain	2570
K_{pi}	Current controller Proportional Gain	0.8

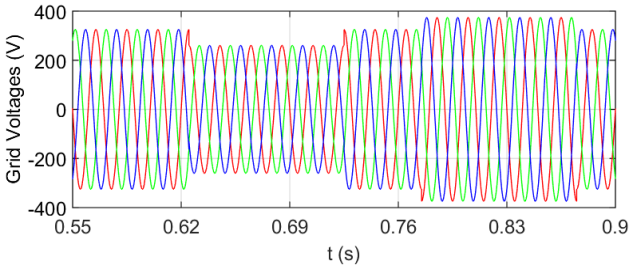

a) Grid Voltages

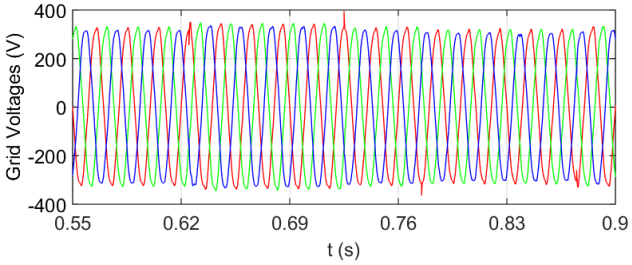

b) Load Voltages

Figure 9. Simulation results of the Voltages

VII. Conclusion

In this paper a UPQC based on an IMC for a PV was proposed. The properties of the UPQC system relative to current harmonics and voltage distortions were maintained, while the system provides another solution to connect the PV to the PCC while keeping the PF unitary. The simulations confirm the properly function of the system within a reasonable time.

References

[1] Axente, I.; Ganesh J.N.; Basu, M.; Conlon, M.F.; Gaughan K.; *A 12-kVA DSP-Controlled Laboratory Prototype UPQC Capable of Mitigating Unbalance in Source Voltage and Load Current*; IEEE Transactions on Power Electronics, Vol. 25, Nº 6, June 2010.

[2] Modesto, R.A.; Silva S.A.; Oliveira A.A.; Bacon V.D.; *A Versatile Unified Power Quality Conditioner Applied to Three-Phase Four-Wire Distribution Systems Using a Dual Control Strategy*; IEEE Transactions on Power Electronics, Vol. 31, Nº8, August 2016.

[3] Kolar, J. W.; Baumann, M.; Schafmeister, F.; Erti, H.; *Novel Three-Phase AC-DC-AC Sparse Matrix Converter*; Proc. IEEE Conference APEC'2002, Volume 2, pp. 777-791, 2002.

[4] Utkin, V.; *Discontinuous Control Systems: State of Art in Theory and Applications*; Proc. IFAC, Munich, July 1987, pp. 75-94.

[5] Holmes, D. G.; Lipo, T. A.; *Implementation of a Controlled Rectifier Using AC-AC Matrix Converter Theory*; IEEE Transactions on Power Electronics, Vol. 7, Nº1, pp. 240-250, January 1992.

[6] Silva, J.; Pires, V.; Pinto, S.; Barros, J.; *Advanced Control Methods for Power Electronics Systems*; Mathematics and Computers in Simulation Vol. 63, IMACS, Elsevier, pp 281-295, 2003.

[7] Jelani, N.; Molinas, M.; *Stability investigation of control system for power electronic converter acting as load interface in AC distribution system*; IEEE 20th International Symposium on Industrial Electronics (ISIE), Gdansk, Poland, June 2011, pp.408-413.

[8] Pinto, S.F.; Mendes, P.V.; Silva, J.F.; *Modular Matrix Converter Based Solid State Transformer for smart grids*; Electric Power Systems Research 136, pp.189-200, 2016.

[9] E. H. Miller, "A note on reflector arrays," *IEEE Trans. Antennas Propagat.*, to be published.

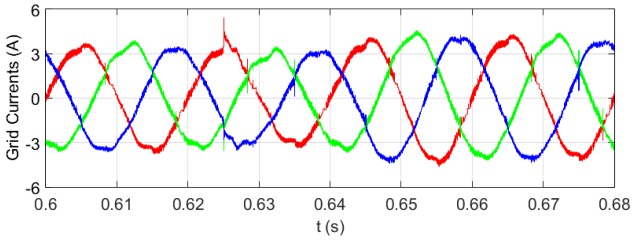

a) Grid currents (sag)

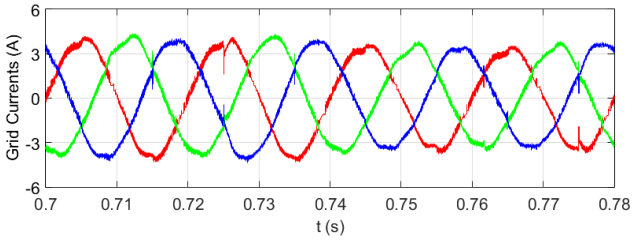

b) Grid currents (swell)

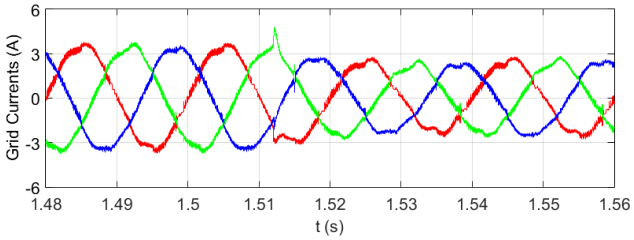

c) Variation of PV parameters

Figure 10. Simulation Results of the Currents